SIMULTANEOUS INVERSION OF RECEIVER FUNCTIONS AND SURFACE-WAVE DISPERSION MEASUREMENTS FOR LITHOSPHERIC STRUCTURE BENEATH ASIA AND NORTH AFRICA

Charles J. Ammon[1], Minoo Kosarian[1], Robert B. Herrmann[2], Michael E. Pasyanos[3], William R. Walter[3], Winchelle Sevilla[1], and George Randall[4]

Penn State University[1], Saint Louis University[2], Lawrence Livermore National Laboratory[3], and Los Alamos National Laboratory[4]

Sponsored by Air Force Research Laboratory
and
National Nuclear Security Administration
Office of Nonproliferation Research and Engineering
Office of Defense Nuclear Nonproliferation

Contract Nos. DE-FC03-02SF22498[1], DTRA01-02-C-0038[2], W-7405-ENG-48[3], and W-7405-ENG-36[4]

ABSTRACT

This paper reports on initial investigations into the seismic structure of the lithosphere in the Middle East and North Africa (MENA) using surface waves and receiver functions. Collections of prior work in the region and computing receiver functions for use in the joint inversion have been initiated. Critical to the joint inversion are surface-wave dispersion information localized to approximately the same region sampled by receiver functions. We continue to improve our surface-wave dispersion model of Western Eurasia and North Africa. We have developed group velocity maps at 2-degree resolution for both Love and Rayleigh waves from 10- to 100-second periods. The model shows excellent relationship to tectonic structure and group velocity variations correlate well with orogenic zones, cratons, sedimentary basins, and rift zones. We have recently implemented a variable-resolution tomography and have pushed the resolution of the model down to 1-degree in areas with sufficient density sampling. We plan to present information on the complexity of receiver structure at many permanent sites in the region and several illustrative inversions for lithospheric structure. We have examined receiver functions at over 200 stations in Eurasia and North Africa and have inverted about 160 using dispersion measurement from global and regional tomographic models. We will present a comparison of crustal thickness and Poisson's ratio estimates for the crust beneath these stations as well as several examples of the joint receiver function surface-wave modeling methodology.

OBJECTIVES

Our objectives are the construction of shear-velocity profiles for regions surrounding broad-band seismic stations throughout Eurasia and central and north Africa (Figure 1). Application of the technique in the region provides an opportunity to revise models of the crust and upper mantle structure throughout the region and to exploit the global and regional work of previous seismic verification research (e.g., Pasyanos et al., 2001; Ritzwoller & Levshin, 1998, Larson and Ekstrom, 2001). The resulting shear-velocity models provide a single structure consistent with a range of observations and which can be tested as a tool for the construction of mode isolation filters that can help improve surface-wave magnitude estimates. We also plan to explore the possibility of adding additional data to our inversions of receiver functions and surface-wave dispersion. The diverse seismic activity throughout the region will facilitate cross-validation of the mode isolation filters with simple empirical filters constructed using larger events with adequate signal-to-noise ratios.

Estimating Subsurface Shear Velocities

Subsurface geology generally has a broad wavenumber spectrum containing spatially localized broadband-wavenumber changes in velocity near Earth's major geologic boundaries and smooth low-wavenumber variations in regions of relatively uniform geologic structure. Access to the full spectrum of earth structure requires that we exploit signals that span a wide frequency range and that are sensitive to the entire spectrum of heterogeneity. Surface-waves, travel times, and direct-wave amplitudes, for example, are sensitive to smooth variations in earth structure; reflected and converted waves are sensitive to velocity contrasts. Combining seismic data in joint inversions is an obvious approach to improve estimates of earth structure. To successfully combine data in an inversion, we must ensure that all the data are sensitive to the same (or related) physical quantities and that they sample or average structure over comparable length scales. Advances in surface-wave tomography have provided an opportunity to combine localized surface-wave dispersion estimates with other data such as P- and S-wave receiver functions.

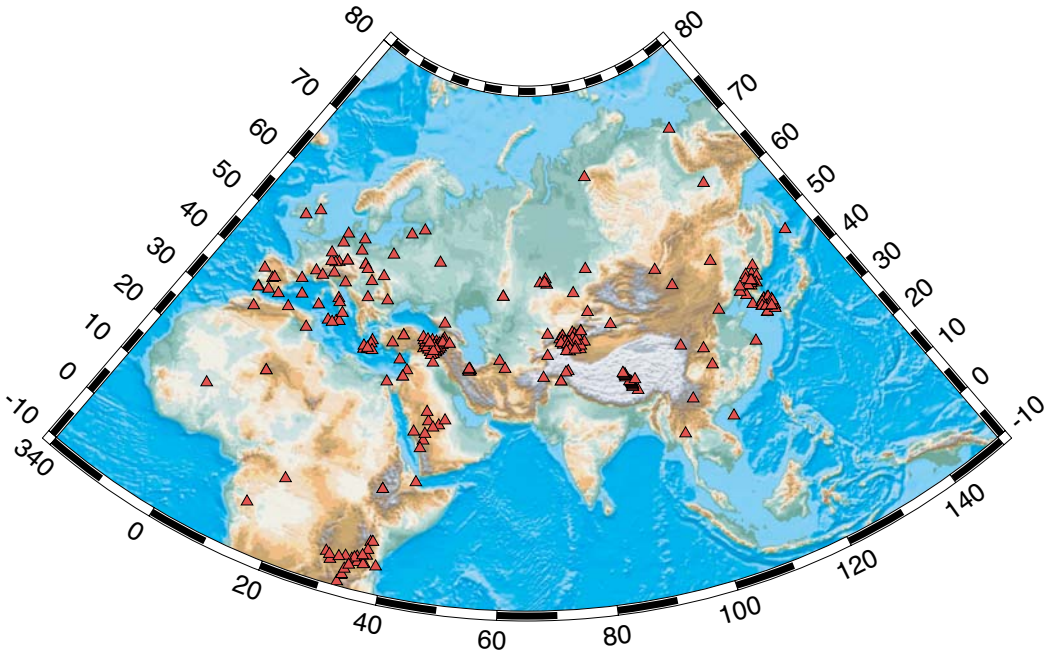

Figure 1. Available permanent and temporary three-component seismic stations in the research area. The data include all readily available permanent and temporary network stations.

Surface-wave dispersion measurements are sensitive to broad averages, or low wavenumber components of earth structure. They provide valuable information on the absolute seismic shear velocity but are relatively insensitive to sharp, high-wavenumber velocity changes. Generally surface-wave inversions must be constrained using a particular layer parameterization (e.g., near-surface, upper-crust, lower crust, mantle lid, deep mantle), resembling an *a priori* model, or substantially smoothed to stabilize earth-structure estimation. Despite these drawbacks, surface-wave dispersion values contain important constraints on the subsurface structure, and the general increase in depth sensitivity with period allows an intuitive understanding of their constraints on structure. Additionally, modeling dispersion values facilitate a broadband inversion by reducing the dominance of Airy phases, which pose problems when constructing broad-band misfit norms to model seismograms directly. Perhaps most important for our application is the ability to localize Earth's dispersion properties using seismic tomography. The idea is now well established and global dispersion models exist for a broad range of frequencies (e.g., Larson and Ekström, 2001; Stevens et al., 2001). The localization of dispersion allows us to isolate the variations in properties spatially and global models of surface-wave dispersion exist and are readily available for application to other studies such as the proposed work.

Receiver functions are time series computed from three-component body-wave seismograms, which show the relative response of Earth structure near the receiver (e.g., Langston, 1979). Source, near-source structure, and mantle propagation effects are removed from the seismograms using a deconvolution that sacrifices P-wave information for the isolation of near-receiver effects (Langston, 1979; Owens et al., 1984; Ammon, 1991; Cassidy, 1992). Receiver function waveforms are a composite of P-to-S (or S-to-P) converted waves that reverberate within the structure near the seismometer. Modeling the amplitude and timing of those reverberating waves can supply valuable constraints on the underlying geology. In general, the receiver functions sample the structure over a range of 10's of kilometers from the station in the direction of wave approach (the specific sample width depends on the depth of the deepest contrast). Stations sited near geologic boundaries can produce different responses for different directions. Recent innovations in receiver function analysis include more detailed modeling of receiver function arrivals from sedimentary basin structures (e.g. Clitheroe et al., 2000), anisotropic structures (e.g. Levin and Park, 1997; Savage 1998), estimation of Poisson's ratio (e.g. Zandt et al., 1995; Zandt and Ammon, 1995; Zhu and Kanamori, 2000, Ligorría, 2000), reflection-like processing of array receiver functions (e.g. Chevrot and Girardin, 2000; Ryberg and Weber, 2000) and joint inversions (e.g. Özalaybey et al., 1997; Du and Foulger, 1999; Julia et al., 2000).

Ammon and Zandt (1993) used surface-wave dispersion observations to try and distinguish between competing models of the Mojave desert, but Özalaybey et al., (1997) pioneered a formal, joint inversion of these data. They nicely illustrated the value of even a limited band of dispersion values to help reduce the trade-off between crustal thickness and velocity inherent in receiver function analyses. Specifically, they used Rayleigh-wave phase velocities in the 20–25 second period range to help produce stable estimates of crustal thickness in the northern and central Basin & Range. The limited bandwidth did not permit resolution of details in the crust and they limited their inversion (or at least their interpretation) to depths above 40 km. More recent authors have exercised the approach and combined the data with additional *a priori* model constraints (Du and Foulger, 1999; Julia et al., 2000). Recent accomplishments in global and regional tomography now provide a more complete band of dispersion measurements to combine with receiver functions that allow us to improve the resolution of earlier works.

Our joint inversion method is similar to that of Özalaybey et al. (1997) except that we use jumping, smoothness, and constraints to include as much *a priori* information into the inversion as is available. We combine the receiver function and surface-wave observations into a single algebraic equation and account for their different physical units and equalize their importance in the misfit norm by weighting each data set by an estimate of the uncertainty in the observations and the number of data. We also append smoothness constraints and *a priori* model constraints on the deepest part of the model. Although we cannot resolve fine details in the deep upper mantle, these regions can impact our results since surface-wave dispersion values at intermediate and longer periods are somewhat sensitive to this deeper structure. We believe that it is important to have a reasonable basement structure so that our results are more consistent with global models. We extend our models to about 500–700 km to insure this consistency. The resulting inversion equations are

$$\begin{bmatrix} \sqrt{\frac{p}{w_s^2}}\mathbf{D_s} \\ \sqrt{\frac{q}{w_r^2}}\mathbf{D_r} \\ \sigma\Delta \\ \mathbf{W} \end{bmatrix} \cdot \mathbf{m_{i+1}} = \begin{bmatrix} \sqrt{\frac{p}{w_s^2}}\mathbf{r_s} \\ \sqrt{\frac{q}{w_r^2}}\mathbf{r_r} \\ 0 \\ 0 \end{bmatrix} + \begin{bmatrix} \sqrt{\frac{p}{w_s^2}}\mathbf{D_s} \\ \sqrt{\frac{q}{w_r^2}}\mathbf{D_r} \\ 0 \\ 0 \end{bmatrix} \cdot \mathbf{m_i} + \begin{bmatrix} 0 \\ 0 \\ 0 \\ \mathbf{W} \end{bmatrix} \cdot \mathbf{m_a} \qquad (1)$$

where $\mathbf{p}$, $\mathbf{q} = 1 - \mathbf{p}$, σ, and $\mathbf{W}$ are weights that control the relative importance of receiver functions, dispersion values, smoothness, and *a priori* model constraints in the norm minimized during the inversion. The data comprise the vectors $\mathbf{r_s}$ and $\mathbf{r_r}$, and the partial derivatives fill the matrices $\mathbf{D_r}$ and $\mathbf{Ds}$. The matrix Δ is a finite-difference stencil that "computes" model roughness, and the matrix $\mathbf{W}$ is a layer-dependent weight that is used to insure the model blends smoothly into the *a priori* model, $\mathbf{m_a}$, at depth. The values of $\mathbf{w_s}$ and $\mathbf{w_r}$ are equal to the product of the number of points in the dispersion curve and receiver functions and the variance of the observations.The second term on the right is added to create the "jumping" inversion scheme (e.g., Constable et al., 1987; Ammon et al., 1990) and allows us to solve for (and constrain) the shear-velocity models as opposed to shear-velocity correction vectors. Equation (1) is solved in a least-squares sense for the model, $\mathbf{m_{i+1}}$, starting with an initial model $\mathbf{m_0}$. The procedure generally converges in a few iterations.

RESEARCH ACCOMPLISHED

Tomographic Imaging of Group-Velocity Variations

We have performed a large-scale study of surface wave group velocity dispersion across Western Eurasia and North Africa (Pasyanos, 2002). This study expands the coverage area northwards relative to previous work (Pasyanos et al., 2001), which covered only North Africa and the Middle East. As a result, we have increased by about 50% the number of seismograms examined and group velocity measurements made. We have now made good quality dispersion measurements for more than 10,000 Rayleigh wave and 6,000 Love wave paths, and have incorporated measurements from several other researchers into the study. We use a conjugate gradient method to perform a group velocity tomography. We have improved our inversion from the previous study by adopting a variable smoothness (Pasyanos, 2002). This technique allows us to go to higher resolution where the data allow without producing artifacts. Our current results include both Love and Rayleigh wave inversions across the region for periods from 10 to 100 seconds. Figure 2 shows inversion results for Rayleigh waves at a period of 35 seconds. Short period group velocities are sensitive to slow velocities associated with large sedimentary features such as the Russian Platform, Mediterranean Sea, and Persian Gulf. Intermediate periods are sensitive to differences in crustal thickness, such as those between oceanic and continental crust or along orogenic zones. At longer periods, we find fast velocities beneath cratons and slow upper mantle velocities along rift systems and the Tethys Belt.

Receiver-Function Estimation

The first step in the project is the selection of target stations and the computation of receiver functions at those stations. To begin, we have a selected a subset of permanent stations that have relatively long recording histories and thus will have substantial data already available. More recently installed stations and operating temporary stations will be added later in the project. Data processed at the time this report was written are shown in Figure 1. We have included all available temporary and permanent stations within central and northern Africa and across much of Eurasia. We have investigated 213 stations: 35 in Africa, 79 in the Middle East, 54 stations in southern Europe, and 45 in eastern Asia.

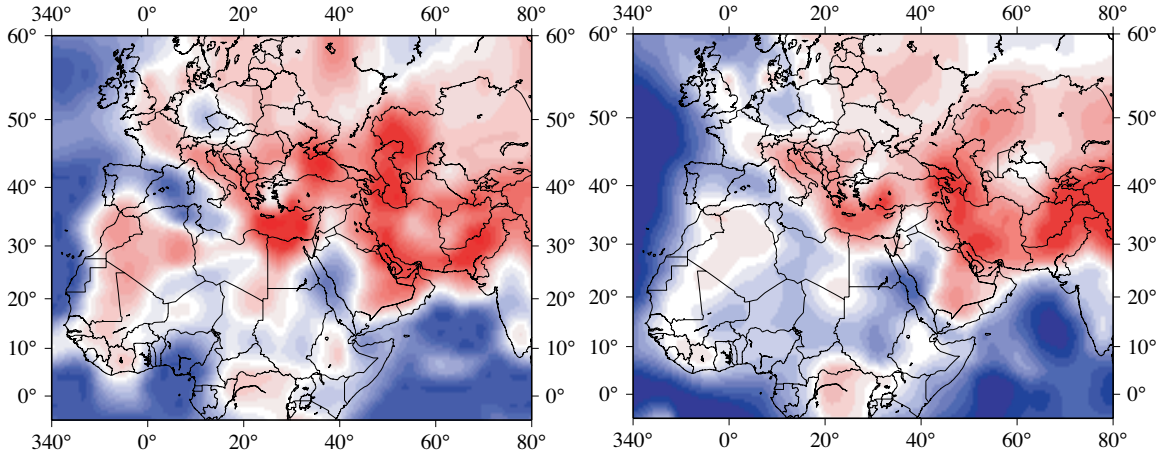

Figure 2. Tomographic imaging results for the Middle East, North Africa, and western Europe. The left diagram shows the lateral group velocity variations in 35-second period Love waves. The map on the right shows the corresponding variations in 35-second period Rayleigh waves. Color scales are relative: blue is fast, red is slow.

Poisson's Ratio and Crustal Thickness Estimation

As a first step in the receiver function analysis we use the receiver function stacking method of Zhu and Kanamori (2000) to estimate the crustal thickness and Vp/Vs velocity ratio (or Poisson's ratio). The stacking method makes a rather limiting assumption of a uniform crust but the analysis provides good estimates of these quantities when the structure is relatively simple. The estimated values of Poisson's ratios can be used in subsequent inversions which require some assumed value of bulk crustal Poisson's ratio. We summarize our results in Figure 3. Although it is difficult to just cluster regions of the continent into simple classifications, we follow Zandt and Ammon (1995) and separate our data into tectonic-age based groups with the exception of Tibet, which we keep as a separate subset of the Mesozoic-Cenozoic regions. Our results are similar to those of Zandt and Ammon (1995) with the exception that our larger survey of shields (including Archean shields) does not show an unusually high Poisson's ratio as was suggested in the earlier data set. Only 7 stations are common to both studies, so the differences are a sampling result. Interestingly, we see no differences between Archean and Proterozoic shields.

Crustal thickness estimates agree on average with the global crustal model 2.0, but at times the differences are significant (greater than 5 km). The mean difference between our results and Crust 2.0 is about 1 km and the standard deviation of the differences is about 7 km, which is larger than the resolution we have on stations with stable receiver functions (probably between 2.5 and 5 km). The crustal thicknesses agree better when we rank our estimates using the complexity of the observed receiver functions.

The Joint Inversion of Receiver Functions and Surface-Wave Dispersion Curves

The receiver function is sensitive to velocity transitions and vertical travel times, surface-wave dispersion measurements are sensitive to averages of the velocities, and relatively insensitive to sharp velocity contrasts. The complementary nature of the signals makes them ideal selections for joint study because they can fill in resolution gaps of each data set. Ammon and Zandt (1993) pointed this out in a study of the Landers region of southern California (although for their specific case, available observations were unsuitable to resolve subtle features in the lower crust) and Özalaybey et al. (1997) and Last et al. (1997) have performed complementary analyses of surface-wave dispersion and receiver functions and Du and Foulger (1999) and Julia et al. (2000) implemented joint inversions of these data types. The mechanics of the inversion are relatively simple since partial derivatives of dispersion observations (Herrmann, 1995) and receiver functions waveforms (e.g., Randall, 1989, Ammon et. al, 1990) can be

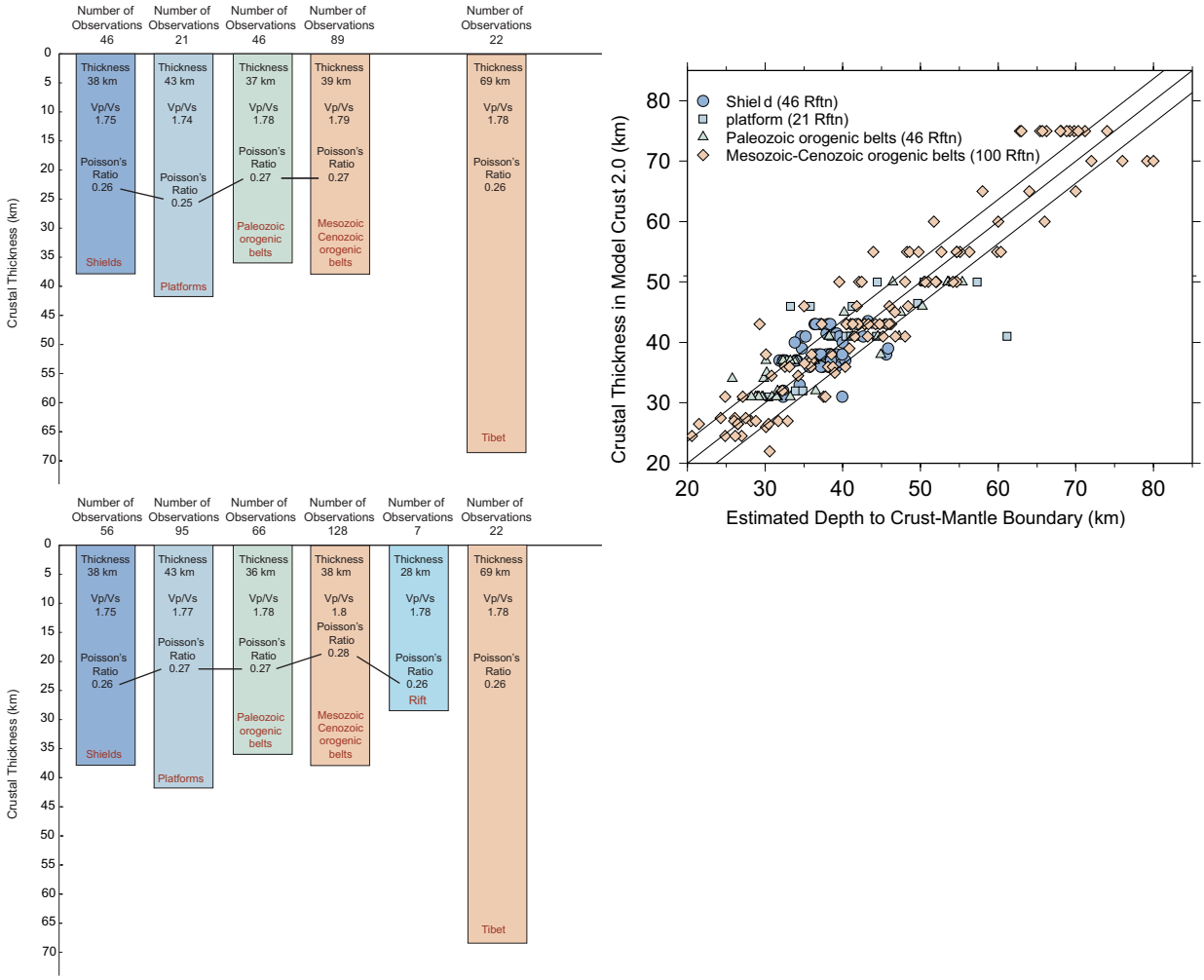

Figure 3. Comparison of crustal thickness estimated with receiver functions in our recent work versus tectonic affiliation. (Top Left) results from this work that include 224 observations; some stations had interpretable receiver functions from more than one azimuth. (Bottom Left) A composite of measurements made during this project and values from the literature. The primary difference is in the platform regions. One would expect a decrease in Poisson's ratio from shield to platform, where the primary geologic difference is in the sediment cover, which tends to lower the Poisson's ratio values. (Top Right) Comparison of crustal thickness estimates from this study and the model Crust 2.0. The results correlate well to first order. Most differences are less than 5 km. Largest differences occur in regions of rapid variations in crustal thickness, where the smooth Crust 2.0 averages across a number of receiver function observation points.

calculated quickly and accurately. Ammon et al. (2004) presented a number of examples, here we present a single example to illustrate the procedure.

An Example Combined Inversion, Station PUGE, Tanzania

We illustrate the ideas with an example. In Figure 4 we present the results of the inversion of PUGE receiver functions with the Rayleigh-wave group-velocity dispersion values from Pasyanos and Walter (2002) combined with phase velocities digitized from Weeraratne et al. (2003). The fit to the Pasyanos and Walter (2002) dispersion curve is very good and the general fit to the phase-velocities is good. The phase velocities are slightly under-predicted for the shorter periods and over-predicted for the longest periods. The long-period over-prediction is a result of our constraints that the deepest part of the model match that of the Prelimninary Reference Earth Model (PREM). Relax-

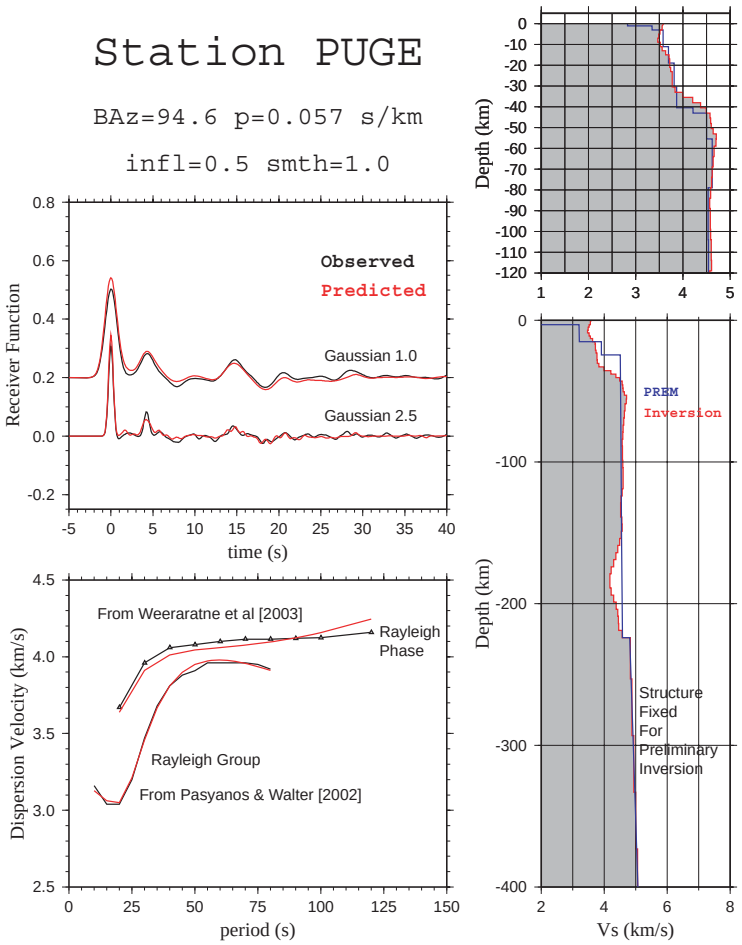

Figure 4. Inversion results for station PUGE using dispersion curves from Pasyanos and Walter (2002) & Weereratne et al., (2003). The back azimuth and ray parameter of the incoming P-wave are shown at the top. The influence parameter was 0.5, which balances the weight between the receiver functions and dispersion values, and the smoothness weight was 1.0. The observed and predicted receiver functions in two bandwidths are shown in the upper left, the observed and predicted dispersion curves in the lower left, and the resulting models are shown on the right. The deep structure is constrained to transition smoothly into the PREM - the data have little sensitivity for detailed absolute velocities below approximately 100-150 km.

ing that assumption would allow the low velocities to extend deeper than 220 km and reduce the deepest average shear-velocity to match the phase velocity. The difference at the shorter periods represents a fundamental difference between the group and phase-velocities. One explanation may be the smoothing of the group velocities has resulted in an artificially lower estimate, very slightly inconsistent with the phase velocities. The receiver functions are very well modeled and produce the relatively smooth crust-mantle transition and crustal thickness (provided with the absolute velocity information from the surface-wave information). The model has a relatively simple crust, consistent with earlier results, and the crust-mantle transition about 7.5 km thick (this could be an intermediate layer at the base of the crust). The mantle structure includes a lid with a thickness of approximately 100 km underlain by a region of low velocities. These velocities are low compared with other shields - consistent with the results of Weeraratne et al (2003). Although the lid is fast at shallow depths, consistent with regional propagation *(*e.g., Nyblade and Brazier, 2002; Langston et al., 2002) the model lid is also thinner than usual for an Archean shield.

CONCLUSIONS AND RECOMMENDATIONS

Our work is concluding nicely. We are refining the results and assessing model performance for waveform matching. In addition to the shear-velocity models, which can act like borehole constraints for smoothed tomography models, our survey has identified a number of seismic stations with exceedingly complicated near-receiver structures that may have an impact on amplitude measurements at those stations.

ACKNOWLEDGEMENTS

We thank P. Wessel and W. H. F. Smith (1991), the authors of GMT for producing easy-to-use, quality software for making maps and charts. We obtained all the data shown in the report through the Incorporated Research Institutions for Seismology Data Management Center.

REFERENCES

Ammon, C. J., G. E. Randall, and G. Zandt (1990), On the non-uniqueness of receiver function inversions, *J. Geophys. Res.* 95: 15303-15318.

Ammon, C. J. (1991), The isolation of receiver effects from teleseismic P waveforms, *Bull. Seism. Soc. Am.* 81: 2504-2510.

Ammon, C. J., and G. Zandt (1993), The receiver structure beneath the southern Mojave Block, *Bull. Seism. Soc. Am.* 83: 737-755.

Ammon, C. J., M. Kosarian, R. B. Herrmann, M. E. Pasyanos, W. R. Walter, and H. Tkalcic (2004), Simultaneous inversion of receiver functions, multi-mode dispersion, and travel-time tomography for lithospheric structure beneath the Middle East and North Africa, in *Proceedings of the 26th Seismic Research Review: Trends in Nuclear Explosion Monitoring,* LA-UR-04-5801, Vol. 1, pp. 17-28.

Cassidy, J. F. (1992), Numerical experiments in broadband receiver function analysis, *Bull. Seismol. Soc. Am.* 82: 1453-1474.

Chevrot, S., and N. Girardin (2000), On the detection and identification of converted and reflected phases from receiver functions, *Geophys. J. Int.* 141: (3), 801-808.

Clitheroe, G., O. Gudmundsson, and B. L. N. Kennett (2000), Sedimentary and upper crustal structure of Australia from receiver functions, *Australian Journal of Earth Sciences* 47: (2), 209-216.

Constable, S. C., R.L. Parker, and C. G. Constable (1987), Occam's inversion: A practical algorithm for generating smooth models from electromagnetic sounding data, *Geophysics* 52: 289-300.

Du, Z .J. and G. R. Foulger (1999), The crustal structure beneath the northwest fjords, Iceland, from receiver functions and surface waves, *Geophys. J. Int.* 139: 419-432.

Herrmann, R. B., *Computer Programs in Seismology*, (1995), St. Louis University, St. Louis, MO.

Julia, J., C. J. Ammon, R. B. Herrmann, and A. M. Correig (2000), Joint Inversion of receiver function and surface-wave dispersion observations, *Geophys. J. Int.* 143: 99-112.

Kikuchi, M., and H. Kanamori, Inversion of complex body waves (1982), *Bull. Seism. Soc. Am.*, 72, 491-506, 1982.

Langston, C.A. (1979), Structure under Mount Rainier, Washington, inferred from teleseismic body waves, *J. Geophys. Res.*, 84, 4749-4762.

Langston, C. A., A. A. Nyblade, and T. J. Owens (2002), Regional wave propagation in Tanzania, East Africa, *J. Geophys. Res.* 107: 1-18.

Larson, E. W. F. and G. Ekström (2001), Global Models of Group Velocity, *Pure and Applied Geophys.* 158: 1377-1399.

Last, R. J., A. A. Nyblade, C. A. Langston, and T. J. Owens (1997), Crustal structure of the East African Plateau from receiver functions and Rayleigh wave phase velocities, *J. Geophys. Res*. 102: 24469-24483.

Levin, V., and J. Park (1997), Crustal anisotropy in the Ural Mountains from teleseismic receiver functions, *Geophysical Research Letters* 24: (11), 1283-1286.

Ligorría, J.P. (2000), An Investigation of the Crust-Mantle Transition Beneath North America and the Bulk Composition of the North American Crust, *Ph.D. Thesis, Saint Louis University*, 261 pages.

Ligorría, J. P. and C. J. Ammon (1999), Iterative deconvolution and receiver function estimation, *Bull. Seismol. Soc. Am.* 89: 1395-1400.

Myers, S. C., and S. L. Beck (1994), Evidence for a local crustal root beneath the Santa Catalina metamorphic core complex, Arizona, *Geology* 22: 223-226.

Nyblade, A. A. and R. A. Brazier (2002), Precambrian lithospheric controls on the development of the East African rift system, *Geology* 30: 755-758.

Owens, T. J., G. Zandt, and S. R. Taylor (1984), Seismic evidence for an ancient rift beneath the Cumberland Plateau, Tennessee: A detailed analysis of broadband teleseismic P waveforms, *J. Geophys. Res.* 89: 7783-7795.

Özalaybey, S., M. K. Savage, A. F. Sheehan, J. N. Louie, and J. N. Brune (1997), Shear-wave velocity structure in the northern Basin and Range Province from the combined analysis of receiver functions and surface waves, *Bull. Seismol. Soc. Am.* 87: 183-199.

Park, J. and V. Levin (2000), Receiver functions from multiple-taper spectral correlation estimates, *Bull. Seismol. Soc. Am.* 90: (6), 1507-1520.

Pasyanos, M. E., W. R. Walter, and S.E. Hazler (2001), A Surface wave dispersion study of the Middle East and North Africa for Monitoring the Comprehensive Nuclear-Test-Ban Treaty, *Pure and Applied Geophys* 158: 1445-1474.

Pasyanos, M. E., and W. R. Walter, Crust and upper-mantle structure of North Africa, Europe and the Middle East from inversion of surface waves, *Geophys. J. Int.* 149: 463-481, 2002.

Pasyanos, M.E. (2002), A Variable-resolution surface wave dispersion Study of Western Eurasia and North Africa, submitted to *Journal of Geophysical Research*.

Ritzwoller, M. H. and A. L. Levshin (1998), Eurasian surface wave tomography: Group velocities, *J. Geophys. Res.* 103: 1839-1878.

Ryberg, T., and M. Weber (2000), Receiver function arrays; a reflection seismic approach, *Geophys. J. Int.* 141: (1), 1-11.

Savage, M.K. (1998), Lower crustal anisotropy or dipping boundaries? Effects on receiver functions and a case study in New Zealand, *J. Geophys. Res.* 103: (7), 15069-15087.

Stevens, J. L. and K. L. McLaughlin (2001), Optimization of Surface Wave Identification and Measurement, *Pure and Applied Geophys*. 158: 1547-1582

Su, W., R. L. Woodward, and A. M. Dziewonski (1994), Degree 12 model of shear velocity heterogeneity in the mantle, *Nature* 99: 6945-6980.

Weeraratne, D.S., D.W. Forsyth, K.M. Fischer, and A.A. Nyblade, Evidence for an upper mantle plume beneath the Tanzanian craton from Rayleigh wave tomography, *J. Geophys. Res.*, 2002JB002273R, 2003.

Wessel, P. and W. H. F. Smith (1991), Free software helps map and display date, EOS, *Trans. of Am. Geophys. Union,* 72: 441-445.

Zandt, G., and C. J. Ammon (1995), Continental Crustal composition constrained by measurements of crustal Poisson's ratio, *Nature* 374: 152-154.

Zandt, G., S.C. Myers, and T.C. Wallace (1995), Crust and mantle structure across the Basin and Range-Colorado Plateau boundary at 37 degrees N latitude and implications for Cenozoic extensional mechanism, *J. Geophys. Res.* 100: (6), 10529-10548.

Zhu, L., and H. Kanamori (2000), Moho depth variation in Southern California from teleseismic receiver functions, *J. Geophys. Res.* 105: (2), 2969-2980.